



Coupling slope-area analysis, integral approach and statistic tests to steady state bedrock river profile analysis

Yizhou Wang, Huiping Zhang, Dewen Zheng, Jingxing Yu, Jianzhang Pang, and Yan Ma

State Key Laboratory of Earthquake Dynamics, Institute of Geology, China Earthquake Administration, Beijing 100029, China

Correspondence to: Yizhou Wang (wangyizhou.-123@163.com)

Abstract. Slope-area analysis and the integral approach both have been widely used in stream profile analysis. However, channel steepness derived from the former one is characterized by large uncertainties and deviated concavities and false knickpoints may occur when utilizing the integral approach. Limited work has been done to couple the advantages of the two methods and remedy such drawbacks. Here we show the merit of the log-transformed slope-area plot to identify colluvial, bedrock and alluvial channels along river profiles. Via the integral approach, we can get bedrock channel concavity and steepness with high precision. In addition, we run bi-variant linear regression statistic tests for the two methods to examine and eliminate serial correlation of residuals. Therefore, the coupled process, combining the advantages of slope-area analysis and the integral approach, can be a more robust and capable method for bedrock river profile analysis.

1 Introduction

Bedrock river profiles record abundant information about tectonics, climatic change, and lithology (Fox et al., 2014, 2015; Goren et al., 2014; Harkins et al., 2007; Royden and Perron, 2013; Snyder et al., 2000). How to retrieve such details has long been debated in both geologic and geomorphologic researches (Flint, 1974; Wobus et al., 2006; Rudge et al., 2015). Most of these studies are based on a well known power-law relationship between local channel gradient and drainage area (Flint, 1974; Hack, 1973; Howard and Kerby, 1983):

$$\frac{dz}{dx} = k_s A^{-\theta} \quad k_s = \left(\frac{U}{K}\right)^{1/n} \quad \theta = \frac{m}{n}, \quad (1)$$

where z is elevation, x is horizontal upstream distance, U is bedrock uplift rate, K is an erodibility coefficient, A is drainage area, and m and n are constants. Parameters θ and k_s are referred to as concavity and steepness indices, respectively. The power-law scaling holds only for drainage areas above a critical threshold, A_{cr} , which is the transition from divergent to convergent topography or from debris-flow to fluvial processes (Montgomery and Foufoula-Georgiou, 1993; Tarboton et al., 1989; Wobus et al., 2006). A growing number of studies have quantitatively mapped steepness to rock uplift (Hu et al., 2010; Kirby and Whipple, 2012; Kirby et al., 2003, 2007; Tarboton et al., 1989). Throughout this paper, we assume a steady state



river profile under constant rock uplift rates and erodibility in time and space. Hence, two forms of solutions to Eq. (1) are derived:

$$\log\left(\frac{U}{k}\right)^{1/n} + \left(-\frac{m}{n}\right)\log A = \log\left(\frac{dz}{dx}\right), \quad (2)$$

$$z = \left(\frac{U}{kA_0^m}\right)^{1/n}\chi \quad \chi = \int_0^x \left(\frac{A_0}{A(x')}\right)^{m/n} dx', \quad (3)$$

- 5 The slope-area analysis, as shown in Eq. (2), yields concavity and steepness indices just by a linear fit to log-transformed slope and area data, which seems to be an easy way to extract fluvial parameters. The colluvial, bedrock and alluvial channels can be identified from the log-transformed slope-area plot, directly (Snyder et al., 2000). However, for its need to estimate slope by differentiating and resampling noisy elevation data, considerable scatter will be typically caused in slope–area plots, making it challenging to identify a power-law trend with adequate certainty (Perron and Royden, 2013). What’s
10 more, the derived channel steepness is doomed to be with high uncertainty owing to error propagation (see details in Sect. 3).

The integral approach, based on an integration of Eq. (1), was proposed by Royden et al (2000) to alleviate such problems by avoiding calculating channel slope. As shown in Eq. (3), the transformed variable χ can be determined directly from drainage area data by simple numerical integration. Based on a proper concavity, the steady state river profile can be converted into a straight line. The slope of the line is steepness (we assume $A_0=1 \text{ m}^2$ throughout the paper). As the best fit
15 value of θ is not known a priori, we can compute χ - z plots for a range of θ values and test for linearity (Perron and Royden, 2013). Thus, this method provides an independent constraint on both θ and k_s (Perron and Royden, 2013). Nevertheless, the uncertainty in k_s will be underestimated for serially correlated residuals. In addition, we may get false concavities and knickpoints for its inability to identify the channel types (see details in Sect. 3).

Based on the analysis above, coupling the advantages of the two methods can make up for their individual drawbacks and
20 provide a better way to constrain stream power parameters. We also run bivariate linear regression statistic tests for the two methods to examine if the residuals of linear fit are homoscedastic and serially correlated. In this paper, we take streams, located in the Mendocino Triple Junction (MTJ) region of northern California (Fig.1), for example, to illustrate the process.

2 Methods

2.1 Coupling slope-area analysis and the integral approach

- 25 A stream usually consists of colluvial, bedrock and alluvial channels. In spite of their complex formation processes, we can identify them from a log-transformed slope-area plot (Fig. 2) (Snyder et al., 2000). The colluvial channel, characterized by steep channel slope ($>20^\circ$) and limited drainage area ($<A_{cr}$) (Wobus et al., 2006), is debris-flow-dominated and beyond the capability of Eq. (1). Both bedrock (detachment-limited) and alluvial (transport-limited) channels show descending gradient with increasing drainage areas, which often exhibit a power-law scaling. However, the alluvial channel is often characterized



by much gentler gradient but a higher concavity (Kirby et al., 2007; Snyder et al., 2000; Whipple and Tucker, 2002), which can be distinguished in the log-transformed plot (Fig. 2).

Via the integral approach (Perron and Royden, 2013), we could get concavities of bedrock channels. Based on a reference concavity index (Hu et al., 2010; Kirby et al., 2003, 2007; Perron and Royden et al., 2013; Snyder et al., 2000; Wobus et al., 5 2006), we then derived the normalized channel steepness indices subject to lower uncertainties.

2.2 Statistic tests

The coupled process does provide a better way to stream profile analysis. However, little has been done to work on the statistic tests of either slope-area analysis or the integral approach. Perron and Royden (2013) noticed the influence of auto-correlated residuals on the steepness uncertainty. In addition, we should make sure that the variance of residuals is a constant 10 (homoscedastic) (Cantrell, 2008; Kirchner, 2001). Here, we introduced Durbin-Watson test (Durbin and Watson, 1950) and Spearman rank correlation coefficient test (Choi, 1977; Fieller et al., 1957; York, 1968) to examine if the residuals are independent and homoscedastic.

2.2.1 Durbin-Watson test

We took the integral approach for an example and rewrote Eq. (3) into another form:

$$15 \quad z_i = z_b + k_s \chi_i + e_i \quad (i = 1, 2 \dots n), \quad (4)$$

In the formula, n is the number of elevation data points, and e represents residuals. We determined the Durbin-Watson (DW) statistics in the following steps:

1) We first calculated the self-correlation coefficient of residuals via Eq. (5):

$$r = \frac{\sum_{i=2}^n e_i e_{i-1}}{\sqrt{\sum_{i=2}^n e_i^2} \sqrt{\sum_{i=2}^n e_{i-1}^2}}, \quad (5)$$

20 2) Then, the DW statistic was derived as: $DW = 2 \times (1 - r)$. Since $-1 \leq r \leq 1$, DW falls in the range of 0-4.

3) We examined if the residuals were auto-correlated according to table 1.

To eliminate the self-correlation, new variables were generated as Eq. (6):

$$z'_i = z_i - r z_{i-1} \quad \chi'_i = \chi_i - r \chi_{i-1} \quad (i = 1, 2 \dots n), \quad (6)$$

Slope of a linear fit to revised relative elevation, z' , and χ' data are channel steepness.

25 2.2.2 Spearman rank correlation coefficient test

To make certain if the residuals variance is a constant, we utilized Spearman rank correlation coefficient test (Choi, 1977; York, 1968):



- 1) Via a linear regression of χ - z plots, we derived the absolute values of residuals $|e|$;
- 2) We sorted the χ values in descending order and recorded the ranks d_{i-1} . Then the χ values were sorted again according to $|e|$ and the new ranks were recorded as d_{i-2} ;
- 3) The Spearman rank correlation coefficient, rs , and the t-statistics, t , were calculated via Eq. (7):

$$rs = 1 - \frac{6}{n(n^2-1)} \sum_{i=1}^n (d_{i-1} - d_{i-2})^2 \quad t = \frac{\sqrt{n-2}}{\sqrt{1-rs^2}} rs \quad (i = 1, 2 \dots n), \quad (7)$$

- 4) When the t value is lower than a threshold, $t_{\alpha/2}(n-2)$, the variance of residuals is a constant. In our example, with $n > 30$ and significance level $\alpha = 0.05$, the threshold value is larger than 2.58.

3 Case study: Mendocino Triple Junction (MTJ) region

Based on 1 Arc-second SRTM DEM, we extracted 15 streams in Mendocino Triple Junction (MTJ) region (Fig. 1). Here we first took streams Cooskie and Juan, for example, to illustrate the advantages and disadvantages of slope-area analysis and the integral approach, as well as to explain why we should couple the two methods.

Stream concavity and steepness indices can be derived from either slope-area analysis or the integral approach. For the same river profile, the two methods should yield identical results (Harkins et al., 2007). We divided the profile of Cooskie stream into colluvial and bedrock channels from the log-transformed slope-area plot (Fig. 3a). The elevation and area of the dividing point are ~ 500 m (Fig. 3b) and 0.1 km^2 (critical area, A_{cr}). The concavity of bedrock channel is $\sim 0.47 \pm 0.05$. We also computed the correlation coefficients between bedrock channel elevation and χ values based on a range of θ . The best linear fit corresponds to $\theta = 0.45$. Both of them are similar to the result (0.43 ± 0.12) of Snyder et al (2000), but a little different with the result (0.36) of Perron and Royden (2013), which may be attributed to the difference in DEM (digital elevation model) resolution or choosing different critical areas.

Although the concavities derived from the two methods are similar, uncertainties in channel steepness differ a lot. The k_s (79.16 ± 29.35) uncertainty from slope-area analysis is $\sim 40\%$ (Fig. 3a) while that from the integral approach is only $\sim 0.5\%$ (62.81 ± 0.39) (Fig. 3d). In addition to smoothing and re-sampling of elevation data, we attribute such large uncertainty to error propagation. The natural logarithmic value of steepness from slope-area analysis is 4.37 ± 0.37 , which results in a k_s value of 79.16 ± 29.35 . It means that the steepness indices will have large uncertainties even for high linear correlation of the log-transformed slope-area plot. Hence, the integral approach is much better for calculating channel steepness.

Nevertheless, for the integral approach, it is often difficult to recognize bedrock and alluvial channels along a river profile. Taking Juan River, for example, we identified colluvial (drainage area $< 0.16 \text{ km}^2$, elevation > 700 m), bedrock and alluvial (drainage area $> 8.89 \text{ km}^2$, elevation < 150 m) channels from the log-transformed slope-area plot (Figs. 4a and b). According to the proper bedrock channel concavity derived from the integral approach ($\theta = 0.52$, Fig. 4c), the bedrock channel profile is converted into a straight line (Fig. 4d).



However, when computing χ - z plots ($A_{cr}=0.16 \text{ km}^2$, both bedrock and alluvial channels) based on a series of concavity values, the best fit θ is 0.72 (Fig. 4e). Then, a knickpoint occurs on the steady state bedrock channel rather than between the bedrock and alluvial reaches. The bedrock channel is divided into two segments with distinct k_s (3354 ± 20 and 1667 ± 15) in the transformed profile (Fig. 4f). Variations in the slope of χ - z plot may be treated as spatially or temporarily variant rock uplift rates (Goren et al., 2014; Perron and Royden, 2013; Royden and Perron, 2013). Since stream power parameters will be misunderstood when using the integral approach alone, we should couple the two methods for river profile analysis.

According to the log-transformed slope-area plots, we identified bedrock channels of the 15 streams. We calculated their concavity indices via both slope-area analysis and the integral approach. As shown by Fig. 5, both of them yielded similar concavities. Based on a mean θ value (0.45), we computed χ - z plots and normalized steepness indices (k_{sn}) with uncertainty estimates (Fig. 6).

We run statistic tests (Durbin-Watson test and Spearman rank correlation coefficient test) for the integral approach and slope-area analysis. For the integral approach, all the DW statistics are lower than D_L (Fig. 7a), indicating serially correlated residuals. Then, we revised the elevation and χ data according to Eq. (6), which is shown in Fig. 8. The DW statistics of revised χ - z plots are all between D_U and $4-D_U$ (Fig. 7a), indicating independent residuals. The results of linear fit are shown in Fig. 8. Although the revised steepness values are similar to the former, estimates of uncertainty are nearly four times to previous ones. For slope-area analysis, the DW statistics are all between D_U and $4-D_U$ (Fig. 7b), showing no auto-correlation.

We also calculated t-statistics for both slope-area analysis and the integral approach (Figs. 7a and b). All of them are no more than 2, indicating homoscedastic residuals.

In addition to statistic tests, another way proposed by Perron and Royden (2013) to estimate uncertainty in steepness is to make multiple independent calculations of different river profiles. From Fig. 6, the mean k_{sn} of high uplift zone ($U=4\text{mm/yr}$) is 104.40 ± 14.06 , and that of low uplift zone ($U=0.5\text{mm/yr}$) is 71.25 ± 10.08 . The standard errors of the mean k_{sn} among profiles are considerably larger than that for individual streams. However, for multiple profiles under similar geological and/or climatic settings, this approach should provide more meaningful estimates of uncertainty.

4 Discussion

Combining slope-area analysis, the integral approach and statistic tests, this coupled method thus is a more robust and reliable method to stream profile analysis. However, Perron and Royden (2013) noticed that the concavity uncertainty resulted from slope-area analysis described how precisely one can measure slope rather than the precision of parameters known for a given landscape. They suggested that the difference between θ values that best linearize the main stem profile and that maximize the co-linearity of the main stem with its tributaries could be an estimate of uncertainty in θ for an individual drainage basin.

In most cases, the θ value that collapses the main stem and its tributaries is often used as a reference concavity (Perron and Royden, 2013; Willett et al., 2014; Yang et al., 2015). In fact, supposing a drainage basin under uniform geologic and



climatic settings, this kind of θ value can be compared with the mean value of concavities of the stem and its tributaries. We call the two kinds of concavities θ_{Co} and θ_{mR} , respectively.

We extracted the stems and tributaries of streams, Singley, Davis, Fourmile and Cooskie (Fig. 9a), based on A_{cr} of 0.1-0.16 km² (Fig. 5). We calculated the correlation coefficients of χ -z plots based on a range of θ (Figs. 9b-d). Then, the θ_{mR} of catchments are 0.45, 0.48, 0.43, and 0.55. We also derived θ_{Co} which collapses the stem and tributaries, 0.45, 0.45, 0.45, and 0.55 (Fig. 10). Both θ_{Co} and θ_{mR} are similar to the stem concavities, 0.50, 0.42, 0.50, and 0.45 (Fig. 5). Hence, for steady state bedrock channels under uniform lithology and precipitation rates, all three kinds of concavities should be similar. Then, the difference between these θ values could be an estimate of concavity uncertainty.

However, it is different for streams consisting of both bedrock and alluvial channels. We extracted the stems and tributaries of streams, Hardy, Juan, Howard and Dehaven (Fig. 11a). The θ_{mR} values of them are 0.57, 0.68, 0.73, and 0.73 (Figs. 11b-e), which are similar to the stem concavities (0.63, 0.70, 0.72, and 0.75) (Figs. 11b-e), but larger than the θ_{Co} (0.45, 0.45, 0.45, and 0.55) (Fig. 12). In such case, differences between θ_{Co} and θ_{mR} are not random errors and cannot be estimates of concavity uncertainty.

Nevertheless, θ_{Co} values (0.45, 0.45, 0.45, and 0.55) are similar to the concavities of bedrock reaches of stems (0.55, 0.52, 0.55, and 0.40) (Fig. 5). Then, the differences between θ_{Co} and concavities of bedrock reaches may be estimates of uncertainties in θ . Hence, the reference concavity collapsing the stem and its tributaries works well even for complex channels consisting of both bedrock and alluvial channels.

In most cases, a somewhat higher constant critical area (e.g. 1 or 5 km²) is assumed to calculate χ values of fluvial channels (Goren et al., 2014, 2015; Willett et al., 2014; Yang et al., 2015). Here we extracted streams of four drainages (Fig. 13a), Hardy, Juan, Howard, and Dehaven, based on a critical area of 0.5km² (three or four times the actual values). We then derived the concavities that best linearize stems (0.73, 0.78, 0.82, and 0.84) (Figs. 13b-e), θ_{mR} (0.60, 0.80, 0.75, and 0.75) (Figs. 13b-e), and θ_{Co} (0.40, 0.50, 0.45, and 0.55) (Fig. 14), respectively. All the results are similar to those based on actual critical areas (Figs. 11 and 12). Hence, choosing a uniform A_{cr} somewhat different to the actual values might be reasonable and would not have significant influence.

5 Conclusion

In this contribution, we coupled the advantages of slope-area analysis and the integral approach to steady state bedrock river profile analysis. First, we identified colluvial, bedrock and alluvial channels from a log-transformed slope-area plot. Utilizing the integral approach, we then derived concavity and steepness indices of a bedrock channel. Finally, via Durbin-Watson statistic test, we examined and eliminated serial correlation of linear regression residuals, which produced more reliable and robust estimates of uncertainties in stream power parameters.



Acknowledgement

We thank Dr. Eric Kirby (Oregon State University) and Dr. Liran Goren (Ben-Gurion University of the Negev) for significant suggestions on slope-area analysis and the integral approach, respectively. We thank Amanda (Oregon State University) and Qi Ou (University of Cambridge) for revision in English writing. We are grateful for the grants from the Strategic Priority Research Program of the Chinese Academy of Sciences (XDB03020200), and from the National Science Foundation of China (41272215, 41272196, 41590861, 41661134011). YW is also funded by state special supporting plan.

References

- Cantrell, C. A.: Technical Note: Review of methods for linear least-squares fitting of data and application to atmospheric chemistry problems, *Atmos. Chem. Phys.*, 8, 5477–5487, doi:10.5194/acp-8-5477-2008, 2008.
- 10 Champagnac, J.-D., Molnar, P., Sue, C., and Herman, F.: Tectonics, climate, and mountain topography, *J. Geophys. Res.*, 117, B02403, doi: 10.1029/2011JB008348, 2012.
- Choi, S. C.: Tests of Equality of Dependent Correlation Coefficients, *Biometrika*, 64, 645–647, doi:10.1093/biomet/64.3.645, 1977.
- Durbin, J., and Watson, G. S.: Testing for Serial Correlation in Least Squares Regression: I, *Biometrika*, 37, 409–428, doi: 10.2307/2332391, 1950.
- 15 Fieller, E. C., Hartley, H. O., and Pearson, E. S.: Tests for rank correlation coefficients. I, *Biometrika*, 44: 470–481, doi:10.1093/biomet/44.3-4.470, 1957.
- Flint, J. J.: Stream gradient as a function of order, magnitude, and discharge, *Water Resour. Res.*, 10, 969–973, doi: 10.1029/WR010i005p00969, 1974.
- Fox, M., Bodin, T., and Shuster, D. L.: Abrupt changes in the rate of Andean Plateau uplift from reversible jump Markov Chain Monte Carlo inversion of river profiles, *Geomorphology*, 238, 1–14, doi:10.1016/j.geomorph.2015.02.022, 2015.
- 20 Fox, M., Goren, L., May, D. A., and Willett, S. D.: Inversion of fluvial channels for paleorock uplift rates in Taiwan, *J. Geophys. Res.-Earth*, 119, 1853–1875, doi:10.1002/2014JF003196, 2014.
- Goren, L., Castelltort, S., and Klinger, Y.: Modes and rates of horizontal deformation from rotated river basins: Application to the Dead Sea fault system in Lebanon, *Geology*, 43, 843–846, doi:10.1130/G36841.1, 2015.
- 25 Goren, L., Fox, M., and Willett S.D.: Tectonics from fluvial topography using formal linear inversion: Theory and applications to the Inyo Mountains, California, *J. Geophys. Res.-Earth*, 119, 1651–1681, doi: 10.1002/2014JF003079, 2014.
- Hack, J. T.: Stream profile analysis and stream-gradient index, *Jour. Research U.S. Geol. Survey*, 1, 421–429, 1973.
- Harkins, N., Kirby, E., Heimsath, A., Robinson, R., and Reiser, U.: Transient fluvial incision in the headwaters of the Yellow River, northeastern Tibet, China, *J. Geophys. Res.*, 112, F03S04, doi:10.1029/2006JF000570, 2007.
- 30 Howard, A. D., and Kerby, G.: Channel changes in badlands, *Geol. Soc. Am. Bull.*, 94, 739–752, 1983.
- Hu, X., Pan, B., Kirby, E., Li, Q., Geng, H., and Chen, J.: Spatial differences in rock uplift rates inferred from channel steepness indices along the northern flank of the Qilian Mountain, northeast Tibetan Plateau, *Chin. Sci. Bull.*, 55, 3205–3214, 2010.
- Kirby, E., and Whipple, K.X.: Expression of active tectonics in erosional landscapes, *J. Struct. Geol.*, 44, 54–75, doi: 10.1016/j.jsg.2012.07.009, 2012.



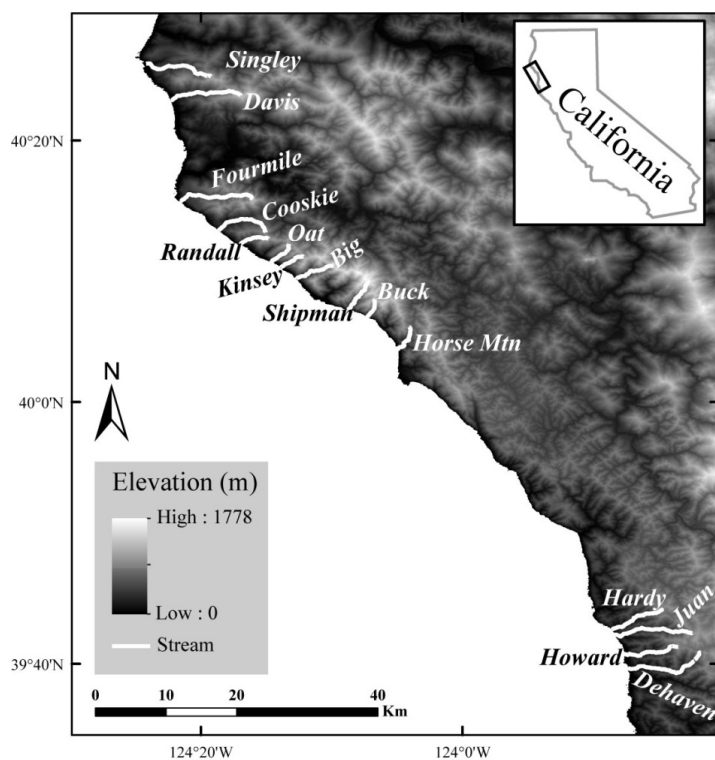
- Kirby, E., Johnson, C., Furlong, K., and Heimsath, A.: Transient channel incision along Bolinas Ridge, California: Evidence for differential rock uplift adjacent to the San Andreas fault, *J. Geophys. Res.*, 112, F03S07, doi:10.1029/2006JF000559, 2007.
- Kirby, E., Whipple, K. X., Tang, W., and Chen, Z.: Distribution of active rock uplift along the eastern margin of the Tibetan Plateau: inferences from bedrock river profiles, *J. Geophys. Res.*, 108, 2217-2240, doi:10.1029/2001JB000861, 2003.
- 5 Kirchner, J. W.: Data Analysis Toolkit #11: Serial Correlation, Course Notes from EPS 120: Analysis of Environmental Data. University of California: Berkeley, CA, available at: http://seismo.berkeley.edu/~kirchner/eps_120/EPSToolkits.htm [20 May 2012], 2001.
- Montgomery, D. R., and Foufoula-Georgiou, E.: Channel network source representation using digital elevation models, *Water Resour. Res.*, 29, 3925-3934, 1993.
- Perron, J. T., and Royden, L. H.: An Integral Approach to Bedrock River Profile Analysis, *Earth Surf. Process. Landforms*, 38, 570-576,
10 doi: 10.1002/esp.3302, 2013.
- Royden, L. H., and Perron, J. T.: Solutions of the stream power equation and application to the evolution of river longitudinal profiles, *J. Geophys. Res.- Earth Surface*, 118, 497-518, 2013.
- Royden, L. H., Clark, M. K., and Whipple, K. X.: Evolution of river elevation profiles by bedrock incision: analytical solutions for transient river profiles related to changing uplift and precipitation rates, *EOS, Transactions of the American Geophysical Union* 81: Fall Meeting
15 Supplement, Abstract T62F-09, 2000.
- Rudge, J. F., Roberts, G. G., White, N. J., and Richardson, C. N.: Uplift histories of Africa and Australia from linear inverse modeling of drainage inventories, *J. Geophys. Res.- Earth*, 120, 894-914, doi:10.1002/2014JF003297, 2015.
- Snyder, N. P., Whipple, K. X., Tucker, G. E., and Merritts, D. J.: Landscape response to tectonic forcing: Digital elevation model analysis of stream profiles in the Mendocino triple junction region, northern California, *Geol. Soc. Am. Bull.*, 112, 1250-1263, 2000.
- 20 Tarboton, D. G., Bras, R. L., and Rodriguez-Iturbe, I.: Scaling and elevation in river networks, *Water Resour. Res.*, 25, 2037-2051, doi: 10.1029/WR025i009p02037, 1989.
- Whipple, K. X.: Bedrock rivers and the geomorphology of active orogens, *Annu. Rev. Earth Planet. Sci.*, 32, 151-185, doi: 10.1146/annurev.earth.32.101802.120356, 2004.
- Whipple, K. X., and Tucker, G. E.: Implications of sediment-flux-dependent river incision models for landscape evolution, *J. Geophys. Res.-Sol. Ea.*, 107, ETG3-1-ETG3-20, doi: 10.1029/2000JB000044, 2002.
- 25 Willett, S. D., McCoy, S. W., Perron, J. T., Goren, L., and Chen, C. Y.: Dynamic reorganization of river basins, *Science*, 343, 1248765, doi: 10.1126/science.1248765, 2014.
- Wobus, C., Whipple, K. X., Kirby, E., Snyder, N., Johnson, J., Spyropolou, K., Crosby, B., and Sheehan, D.: Tectonics from topography: Procedures, promise, and pitfalls, in: *Tectonics, climate, and landscape evolution*, edited by: Willett, S. D., Hovius, N., Brandon, M. T., and Fisher, D. M., *GSA Special Paper*, 398, Penrose Conference Series, 55-74, doi: 10.1130/2006.2398(04), 2006.
- 30 Yang, R., Willett, S. D., and Goren, L.: In situ low-relief landscape formation as a result of river network disruption, *Nature*, 520, 526-529, doi:10.1038/nature14354, 2015.
- York, D.: Least squares fitting of a straight line with correlated errors, *Earth Planet. Sci. Lett.*, 5, 320-324, doi:10.1016/S0012-821X(68)80059-7, 1968.



Table 1. Range of DW statistic and the related meaning

DW Statistic	Meaning
$0 \leq DW \leq D_L^*$	Positively auto-correlated residuals
$D_L^* < DW \leq D_U^*$	Beyond the suitability of Durbin-Watson test
$D_U^* < DW < 4 - D_U$	Mutually independent residuals
$4 - D_U \leq DW < 4 - D_L$	Beyond the suitability of Durbin-Watson test
$4 - D_L \leq DW \leq 4$	Negatively auto-correlated residuals

* D_L and D_U represent the critical value of Durbin-Watson test and can be found in Durbin and Watson (1950).



5

Figure 1. Streams in the Mendocino Triple Junction (MTJ) region of northern California, USA. Streams are from Snyder et al (2000). The elevation data are from 1 Arc-Second SRTM (<http://earthexplorer.usgs.gov/>)

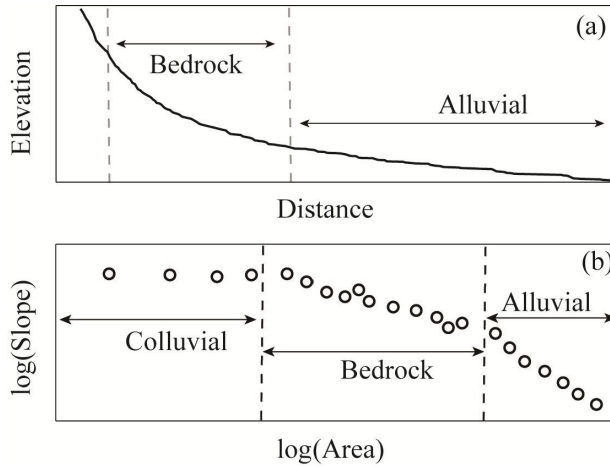
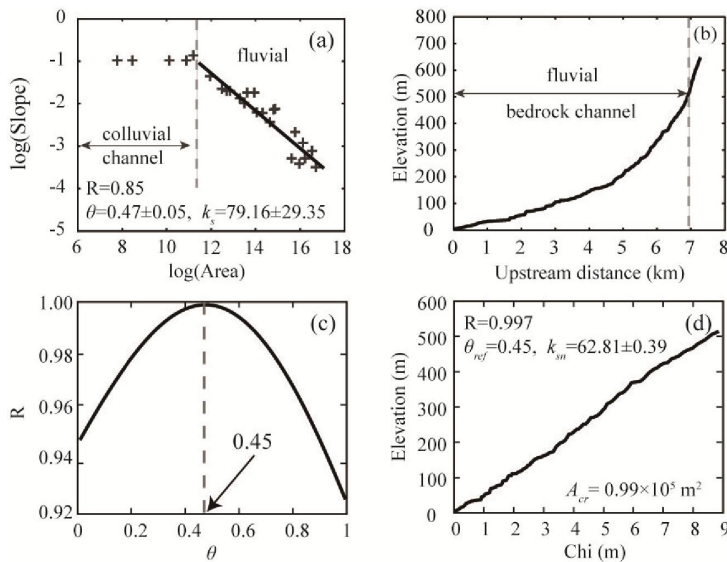


Figure 2. Schematic of a steady state river profile consisting of colluvial, bedrock and alluvial channels, revised from Figures 7A and B in Snyder et al (2000). (a) Stream profile. (b) Log-transformed slope-area plot.



5

Figure 3. Stream profile analysis of Cooskie. (a) Log-transformed slope-area plot. The slope was derived from the smoothed (horizontal distance of 300m) and re-sampled (elevation interval of 20m) elevation data. (b) The full river profile (without any smoothing or re-sampling) of Cooskie. (c) The correlation coefficients, R , as a function of θ for least-squares regression based on Eq. (3). The maximum value of R , which corresponds to the best linear fit, occurs at $\theta=0.45$ (dotted line and black arrow). (d) χ - z plot of the bedrock channel profile, transformed according to Eq. (3) with $\theta=0.45$, $A_{cr}=0.1 \text{ km}^2$, and $A_0=1 \text{ m}^2$.

10

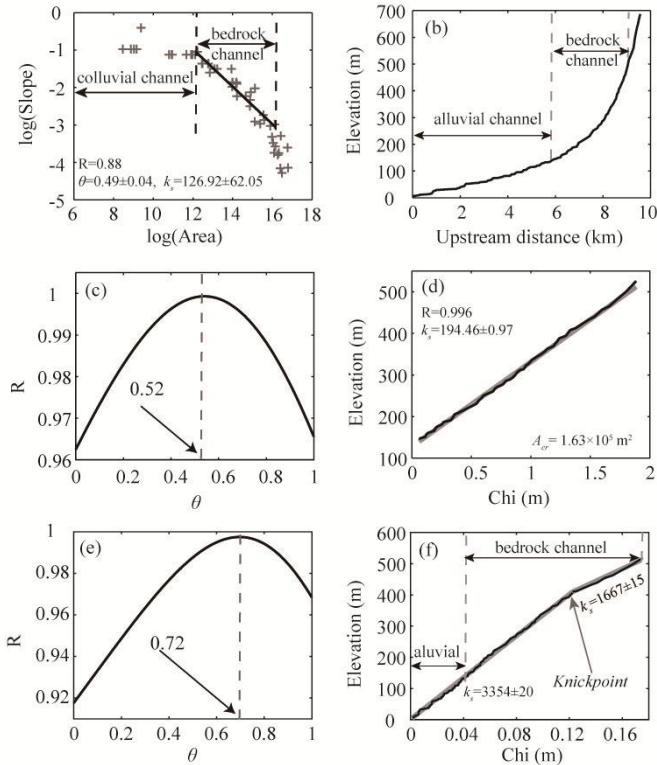


Figure 4. Stream profile analysis of Juan. (a) Log-transformed slope-area plot. The slope was derived from the smoothed (horizontal distance of 300m) and re-sampled (elevation interval of 20m) elevation data. (b) The full river profile (without any smoothing or re-sampling) of Juan. (c) The correlation coefficients of χ - z plots as a function of θ for bedrock channels. The maximum value of R occurs at $\theta=0.52$. (d) χ - z plot of the bedrock channel profile based on a concavity value of 0.52. (e) The correlation coefficients of χ - z plots as a function of θ for fluvial (both bedrock and alluvial) channel. The maximum value of R occurs at $\theta=0.72$. (f) χ - z plot of the fluvial (both bedrock and alluvial) channel profile based on a concavity value of 0.72.

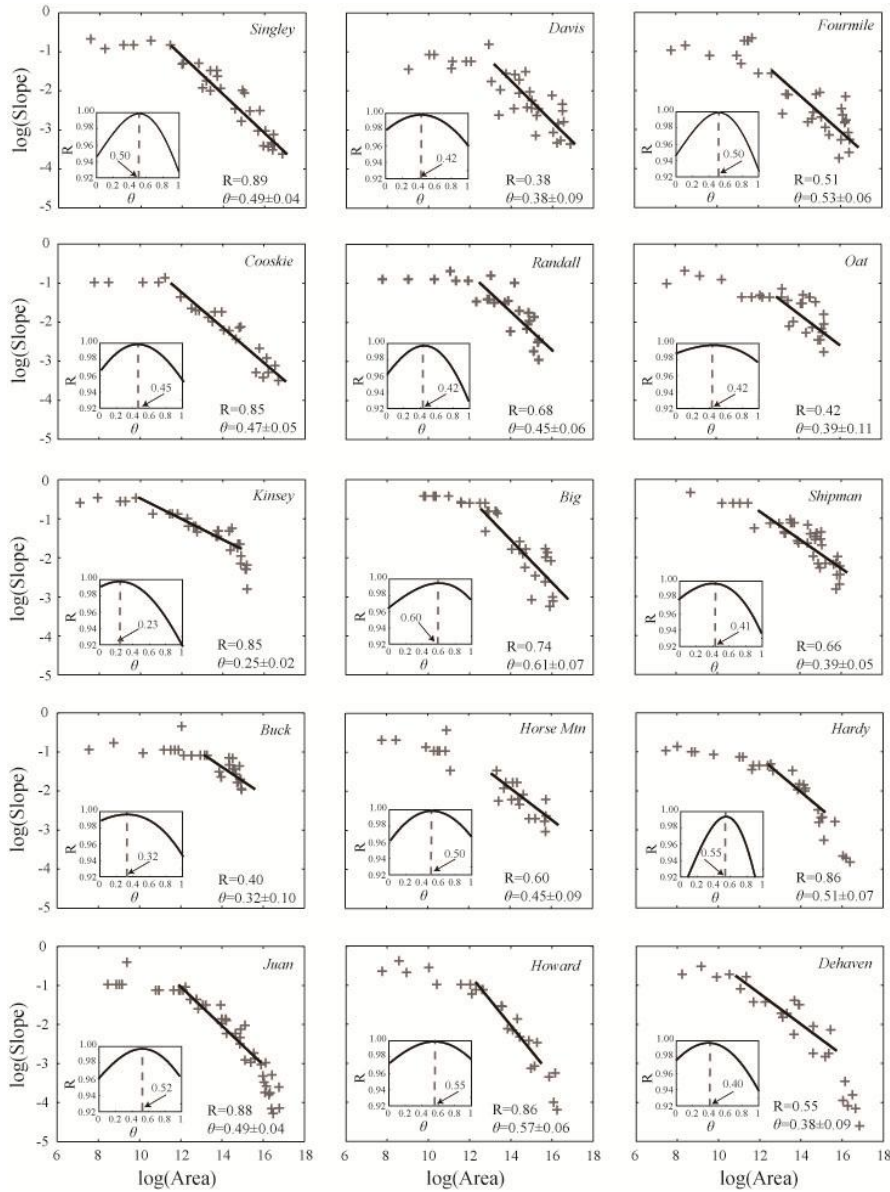


Figure 5. Correlation coefficients derived from slope-area analysis and the integral approach. The slope was derived from the smoothed (horizontal distance of 300m) and re-sampled (elevation interval of 20m) elevation data. The correlation coefficients of χ -z plots as a function of θ for bedrock channels are shown in the left bottom. Then mean θ value is 0.45.

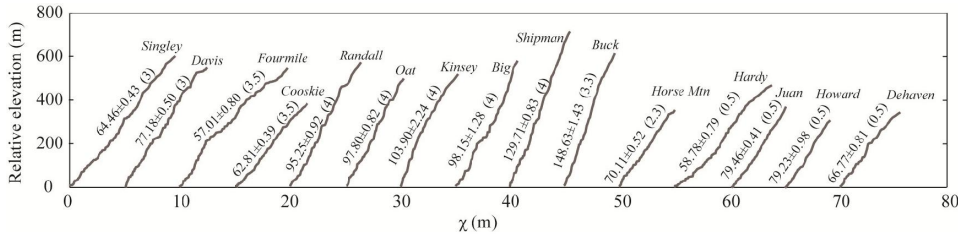


Figure 6. χ - z plots of the streams (bedrock channels) based on the mean concavity (0.45). Numbers are normalized channel steepness, k_{sm} , with the uncertainty estimates. Numbers in the parentheses are uplift rates with a unit of millimeter per year (Snyder et al., 2000). Italic characters are stream names.

5

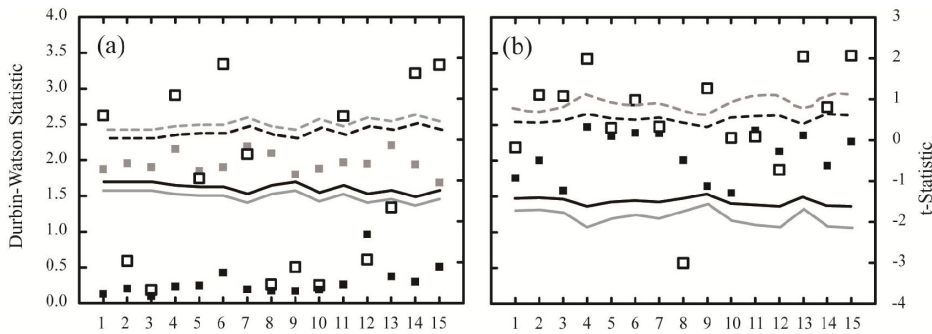


Figure 7. Statistic tests for the integral approach (a) and slope-area analysis (b). Black hollow squares are t-statistic of Spearman rank correlation coefficient. Black solid squares are Durbin-Watson statistics. The gray solid line, black solid line, black dashed line and gray dashed line are D_L , D_U , $4-D_U$ and $4-D_L$. Gray squares in Figure (a) are the Durbin-Watson statistics of revised χ - z plots. The river numbers 1 to 15 indicate streams: Singley, Davis, Fourmile, Cooskie, Randall, Oat, Kinsey, Big, Shipman, Buck, Horse Mtn, Hardy, Juan, Howard, and Dehaven.

10

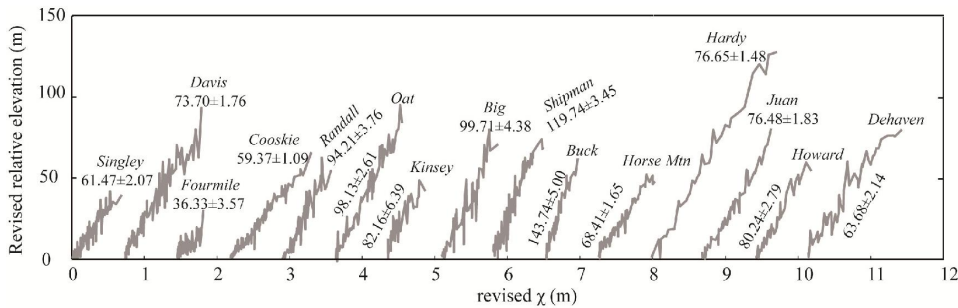


Figure 8. Revised relative elevation and χ values. Gray lines and Numbers are revised data and steepness index with uncertainty estimates.

15

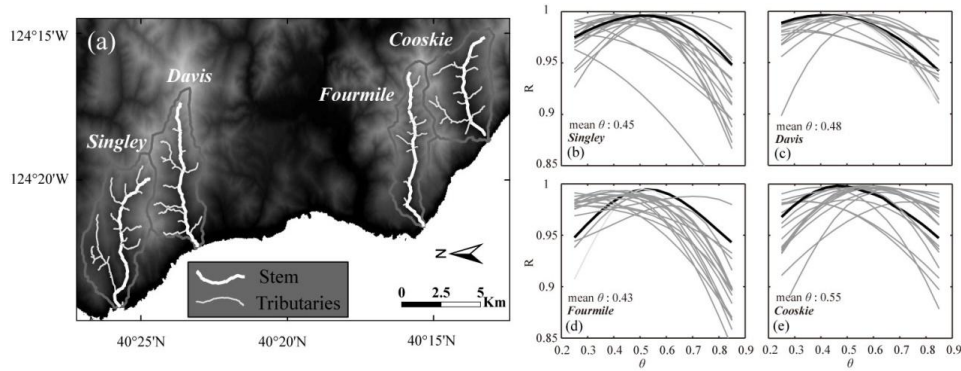


Figure 9. Correlation coefficients of χ - z plots as a function of θ . (a) Location of the streams. (b-e) Correlation coefficients of χ - z plots based on a range of θ values. Black thick lines indicate stems.

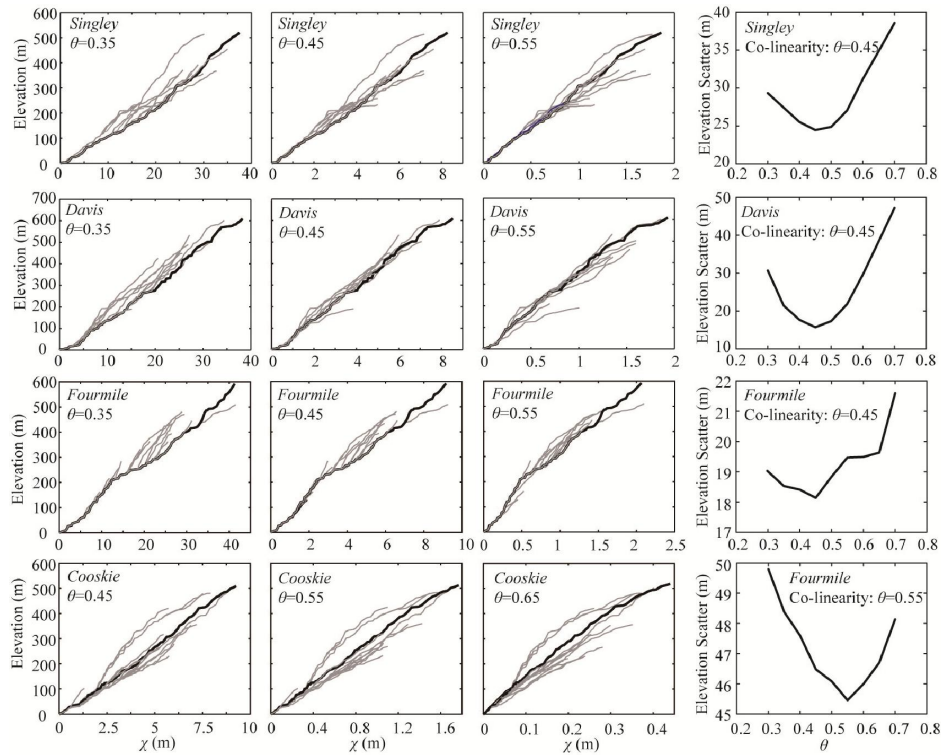


Figure 10 Concavity values that maximize the co-linearity of the main stem with its tributaries. Black thick lines in the χ - z plots are stems.

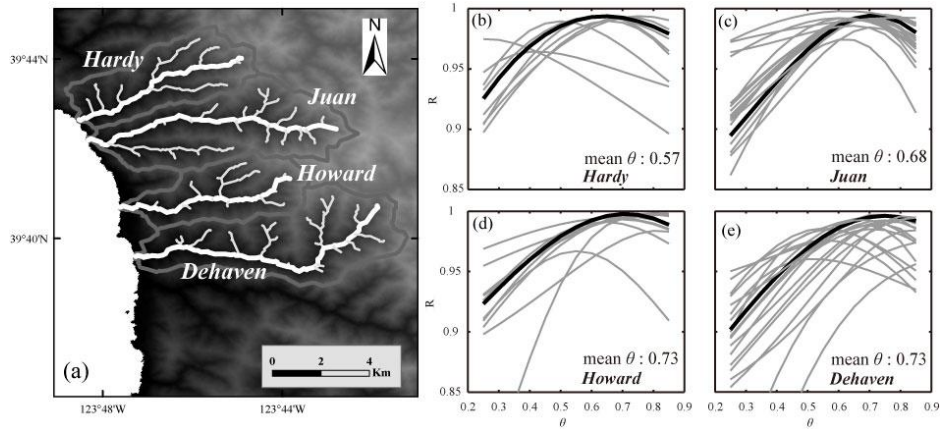


Figure 11. Correlation coefficients of χ - z plots as a function of θ . (a) Location of the streams. (b-e) Correlation coefficients of χ - z plots based on a range of θ values. Black thick lines indicate stems.

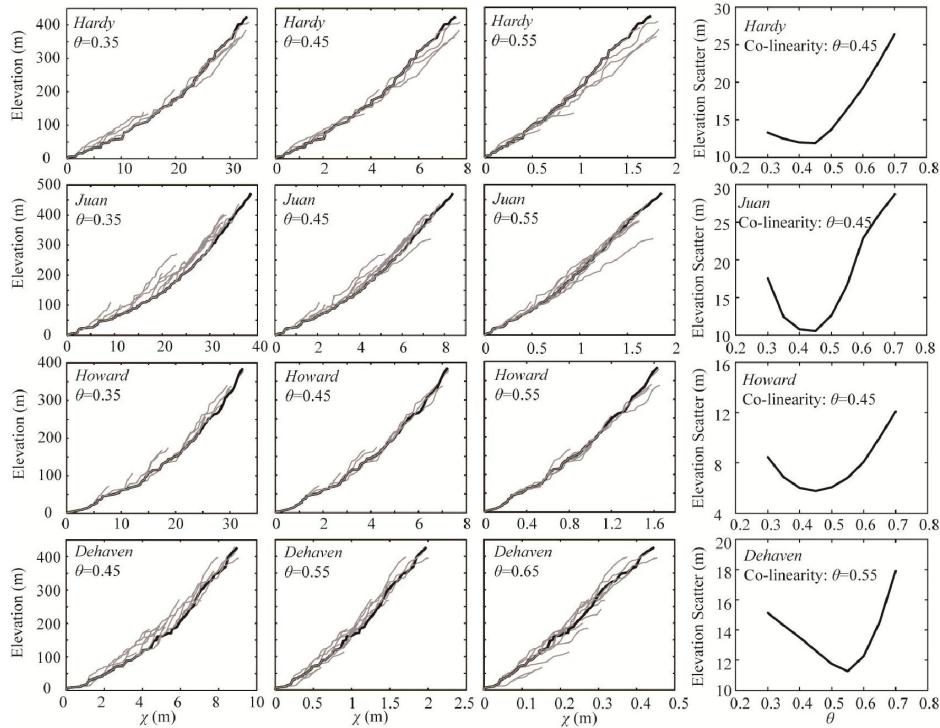


Figure 12. Concavity values that maximize the co-linearity of the main stem with its tributaries. Black thick lines in the χ - z plots are stems.

5

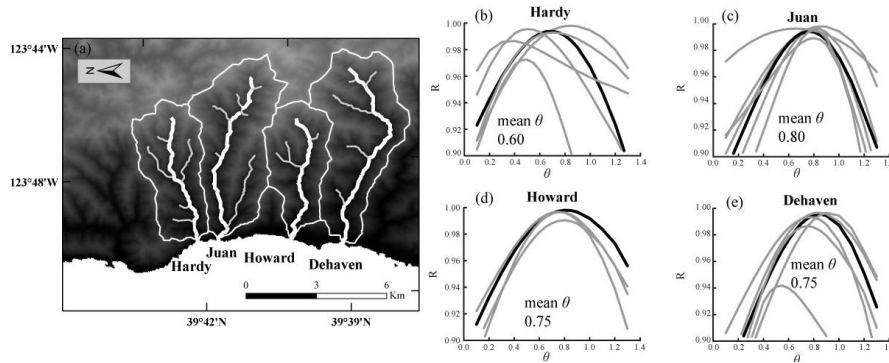


Figure 13. Correlation coefficients of χ - z plots as a function of θ . (a) Location of the streams. Streams are extracted with a critical area of 0.5km^2 . (b-e) Correlation coefficients of χ - z plots based on a range of θ values. Black thick lines indicate stems.

5

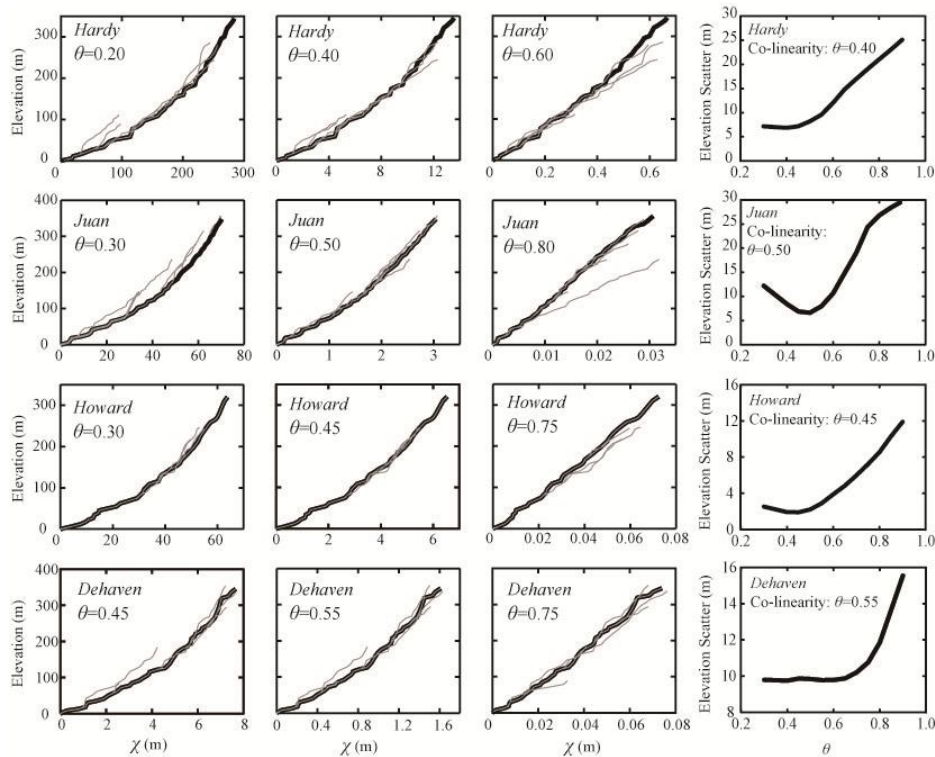


Figure 14. Concavity values that maximize the co-linearity of the main stem with its tributaries. Black thick lines in the χ - z plots are stems.